Effect of Processing Conditions on Premature Gelling, Knit Line Strength, and Physical Properties for the RIM Process

J. M. CASTRO, *PLAPIQUI, UNS-CONICET, Bahía Blanca, Argentina*,
C. W. MACOSKO, *Department of Chemical Engineering and Material Science, University of Minnesota, Minneapolis, Minnesota 55455*, and
F. E. CRITCHFIELD, *Union Carbide Corporation, South Charleston, West Virginia 25303*

Synopsis

It is shown how using the relevant dimensionless groups for the RIM process, guidelines for premature gelling, and knit line problems can be achieved. The influence of processing conditions on final plaque physical properties is analyzed. It is shown that RIM parts, due to the fact that most of the polymerization reaction occurs after the mold is filled, are fairly isotropic with respect to planar rotations parallel to the mold walls.

INTRODUCTION

During a RIM molding cycle, two highly reactive monomers or prepolymers (in the case of urethanes a diisocyanate and a polyol–diol mixture), are brought into intimate molecular contact by impingement mixing. From the mixing head they flow into the mold. When the mold is filled, the materials are left in place, reacting (curing) until the part is stiff enough such that it can be removed without losing its shape. During filling, the viscosity of the flowing mixture increases due to chemical reaction. Typical fill times are short; however, the industry trend seems to be toward larger, more complex molds and faster reacting systems.

As RIM molds become larger and more complex, and as more reactive systems are used, understanding the filling step takes on greater importance. Premature gelling has been reported[1,2] to give problems in complex parts. Knit lines are also a potential problem. If the extent of reaction of the fluid streams meeting each other is higher than a critical value, the materials will not interpenetrate and the knit line will be visible and weak. Criteria are needed to predict incomplete filling and knit line problems. To optimize the process, we also need to understand how processing conditions affect the properties of the final product. This relationship is complicated by the presence of the chemical reaction. The exothermic character of the reaction, for example has been shown to create some important spatial variations in RIM urethanes.[3-5]

The purposes of this paper are twofold: first, to show how using the dimensionless groups of the process identified by Castro and Macosko,[6] one can obtain useful criteria for premature gelling and knit line problems and, second, to study the effect of processing conditions on the final part physical properties and their isotropy under typical RIM processing conditions.

TABLE I
Composition of Union Carbide's RIM 2200[a]

Polyol stream	wt %	Isocyanate stream	wt %
Niax polyol 31-23 (long polyol) (polyether polymer polyol M_n = 5000)	85	Isocyanate 143L Liquid form of 4,4'-diphenyl methane diisocyanate	100
1,4-Butane diol (BDO)	15		

[a] Stoichiometric ratio = 1.04, C_{OH_0} = 0.00241 mol/cm^3, ρ = 1 g/cm^3.

EXPERIMENTAL

Materials

Typical urethane RIM type chemical systems consist of a short diol, called the extender (B_2); a long polyol (B_2') and a liquid form of 4,4'-diphenyl methane diisocyanate. The catalyst is usually dibutyltin dilaurate, which is soluble in the reactants. In the present work two systems were used, a commercial one (Union Carbide's RIM 2200) for the knit lines study and a model system[7] for the final plaque physical properties. They differ only in the long polyol. The experimental system uses a simpler, linear polyol. All commercial systems use a polyol with a functionality greater than 2. Their components are shown in Tables I and II. RIM 2200 is representative of commercial automotive fascia formulations. For all cases, the catalyst used was dibutyltin dilaurate. The kinetics and rheology of these chemical systems has been studied by Castro and Macosko.[8]

Procedures

Knit Line Study. The experiments were performed using an end-gated aluminum mold (100 cm × 30.5 cm × variable thickness) equipped with a thermocouple (20-gauge copper constantan-sheathed thermocouple 0.0625 in. O.D. type S.S. sheath length 2.5 in., 35477-102 Marlin Manufacturing Co.) located at about 5 cm from the mold entrance. The thermocouple was introduced through 0.0625 in. hole in the side wall. A commercial RIM machine was used

TABLE II
Composition of Model System[a]

Polyol stream	wt %	Isocyanate stream	wt %
12-56 Experimental (long polyol) polyether polyol (M_n = 2000)	85	Isocyanate 143L	100
1,4-Butane diol (BDO)	15		
12-56: Polypropylene oxide capped with ethylene oxide			

$$\text{HO}(CH_2CH_2O)_a-(\overset{\overset{\displaystyle CH_3}{|}}{CH}CH_2O)_b-(CH_2CH_2O)_cH$$

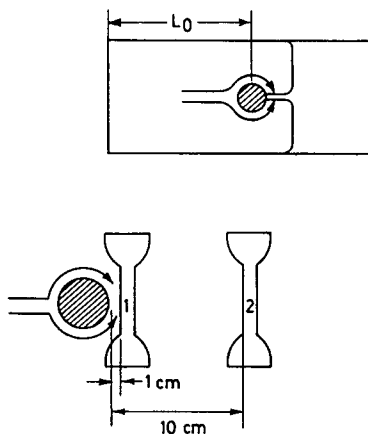[a] Stoichiometric ratio = 1.0, C_{OH_0} = 0.0026 mol/cm^3, ρ = 1 g/cm^3.

Fig. 1. Location of tensile bars for knit line experiments.

(Admiral 900-2HP dual speed, 15–90 lb/min throughput). The polyol temperature was kept close to 60°C and the isocyanate at 27°C. The starting material temperature was taken to be the one measured by the thermocouple near the entrance of the mold. The mold was preheated in an oven to an operating temperature of 48 ± 5°C. The temperature was determined just before filling with a surface thermometer.

A 1-in.-diameter steel cylinder was placed midway between the lateral mold walls and at various distances from the mold entrance. Two tensile bars were cut perpendicular to the flow direction at about 1 cm and 10 cm from the object, as shown in Figure 1. The elongation and tensile stress at failure were determined. The region downstream from the object was examined for visible defects. Conditions for the experiments are summarized in Table III.

Final Plaque Physical Properties. The experiments were done using an aluminum mold (75 cm × 10.1 cm × variable thickness). To fill the mold, a laboratory scale RIM machine designed by Lee and Macosko[9] was used. The materials were degassed for about 2 h before charging them into the machine. The resin and isocyanate temperature were kept close to 60°C and 30°C, respectively. The specific values for each experiment were measured with a Fe–Cu 20-gauge thermocouple located in each of the dispensing cylinders. The initial material temperature was obtained by assuming ideal mixing of both reactants. The mold wall temperature was varied between 27°C and 110°C. For temper-
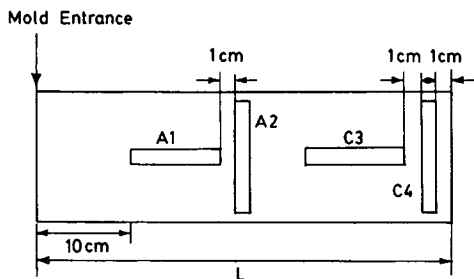

Fig. 2. Location of four samples used for tensile testing.

TABLE III
Experimental Conditions for the Knit Line Experiments[a]

Experiment	1	2	3	4	5	6
L_0 (cm)	58.4	58.4	73.7	73.7	36.83	36.83
Q (cm³/s)	395.9	395.9	415.8	415.8	226.5	226.5
t_0 (s)	2.88	2.88	3.46	3.46	3.17	3.17
T_w (°C)	48.0	48.0	48.0	48.0	48.0	48.0
T_0 (°C)	55.8	56.5	55.2	56.1	54.8	53.2
G_0	0.085	0.086	0.103	0.104	0.090	0.086
G_z	40	40	33.3	33.3	35.7	35.7
σ_b at 1 (Pa × 10^{-6})	10.5	10.3	10.1	11.3	10.9	12.2
ϵ_b at 1	90	90	60	90	140	140
σ_b at 2 (Pa × 10^{-6})	14.0	13.0	14.4	14.9	11.0	11.2
ϵ_b at 2	190	150	150	150	100	100
Qualitative classification	Good	Good	Good	Good	Good	Good
Experiment	7	8	9	10	11	12
L_0 (cm)	36.8	36.8	73.7	96.0	52.1	87.6
Q (cm³/s)	418.8	418.8	603.5	603.5	226.5	418.8
t_0 (s)	1.72	1.72	2.38	3.10	4.49	4.08
T_w (°C)	48.0	48.0	48.0	48.0	48.0	48.0
T_0 (°C)	54.5	53.8	52.9	61.2	57.2	55.4
G_0	0.049	0.047	0.066	0.107	0.138	0.119
G_z	66.67	66.67	47.62	37.04	25.64	28.56
σ_b at 1 (Pa × 10^{-6})	15.4	15.7	15.3	6.1	2.9	<2.9
ϵ_b at 1	190	140	150	40	10	<10
σ_b at 2 (Pa × 10^{-6})	16.0	16.0	13.8	10.0	4.7	—
ϵ_b at 2	200	190	150	90	40	—
Qualitative classification	Very good	Very good	Very good	Fair	Bad	Bad

[a] $H = 0.64$ cm; $W = 30.48$ cm.

atures above 27°C, the mold was preheated in an oven. The mold wall temperature was determined just before filling using a digital thermometer with a surface probe (Markson Model 5650 Probe Model 5655). The experimental conditions are summarized in Table IV.

For the actual experiments, when the machine was ready, the mold was taken out of the oven and connected to the mixing head. The mold was kept closed for about 2 min. After that time, the mold was opened and the part removed. The plaques were then post-cured for about 2 h at 110°C in an oven. For each plaque four samples were tested. The locations of each sample are shown in Figure 2. The properties measured were the modulus at 100% elongation (E_{100}), the ultimate stress (σ_b), and the ultimate elongation (ϵ_b). Some of the plaques were also tested by dynamic torsion (G', G''), in which case the sample was taken from a location equivalent to A2 but from the first 10 cm of the plaque. The dynamic measurements were performed in a Rheometrics dynamical spectrometer (RDS) at a frequency of 1 H and 0.1% strain. The temperature was varied between −100°C and 30°C.

TABLE IV
Physical Properties, Experimental Conditions

Experiment identification	H (cm)	T_0 (°C)	T_w (°C)
9/22/1	0.16	48.8	72.1
9/22/2	0.16	51.8	64.3
9/25/1	0.16	53.1	70.0
8/31/1	0.16	48.9	75.0
9/5/1	0.16	49.8	76.8
9/5/2	0.32	50.5	66.9
9/21/2	0.32	54.0	70.0
8/31/2	0.32	51.2	72.2
9/21/1	0.32	55.3	82.0
9/4/1	0.32	49.3	74.1
9/5/3	0.32	49.9	52.0
L 110	0.32	60.0	110.0
L 67	0.32	60.0	67.0

RESULTS

Knit Line Study

Castro and Macosko[6] have shown that the most important dimensionless group for the filling step is the gelling number. The larger its value, the more the material reacts during filling. The knit line results can be correlated using a local gelling number (G_0) defined as follows:

$$G_0 = \frac{\text{time to fill the mold up to } L_0(t_{f0})}{\text{isothermal gel time at } T_m \ (t_{gm})} \tag{1}$$

where T_m is the average between the mold wall temperature (T_w) and the initial material temperature (T_0) and L_0 is the distance from the knit line up to the entrance of the mold (Fig. 1).
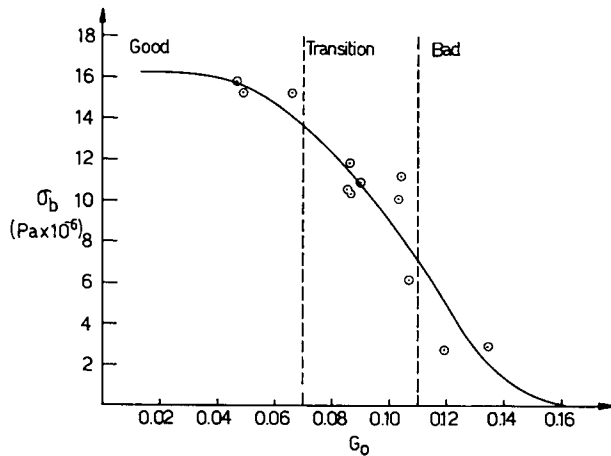
Fig. 3. Knit line strength (σ_b) as a function of gelling number (G_0).

TABLE V
Final Plaque Physical Properties Results

Sample no.		E_{100} (Pa $\times$ 10^{-6})	σ_b (Pa $\times$ 10^{-6})	ϵ_b %
9/22/1	A1	8.3	17.9	290
	A2	8.4	19.2	300
	C3	8.7	16.5	210
	C4	8.3	20.7	225
Average		8.4	16.1	256
9/22/2	A1	7.8	17.9	290
	A2	8.3	18.8	300
	C3	8.6	13.8	210
	C4	8.5	13.8	225
Average		8.3	16.1	256
9/25/1	A1	9.2	15.6	250
	A2	9.2	14.2	240
	C3	8.9	15.6	255
	C4	8.7	11.9	190
Average		9.0	14.3	234
8/31/1	A1	8.4	13.2	260
	C3	7.8	12.5	250
Average		8.1	12.9	255
9/5/1	A1	6.9	11.9	320
	A2	6.8	14.5	405
	C3	6.7	11.1	255
Average		6.8	12.5	326
9/5/2	A1	5.0	12.3	400
	A2	5.2	12.8	390
	C3	5.2	11.9	365
	C4	4.9	13.1	400
Average		5.1	12.5	389
9/21/2	A1	6.6	11.5	225
	A2	6.4	11.3	215
	C3	6.5	11.9	220
	C4	6.4	12.9	255
Average		6.5	11.9	229
8/31/2	A1	6.2	12.1	250
	A2	6.3	10.4	220
	C3	6.3	8.6	170
	C4	6.1	13.5	300
Average		6.2	11.1	235
9/21/1	A1	6.4	10.5	200
	A2	6.2	10.9	205
	C3	6.3	11.8	220
	C4	6.6	9.3	165
Average		6.4	10.6	198
9/4/1	A1	7.0	11.2	250
	A2	7.0	6.9	300
	C3	6.4	10.9	180
	C4	7.2	11.2	190
Average		6.9	10.1	230
9/5/3	A1	5.6	9.4	250
	A2	5.6	10.1	250
	C3	5.6	10.0	255
	C4	5.6	10.5	255
Average		5.6	10.0	253

TABLE VI
Summary of Dynamic Torsion Data

Experimental	H (cm)	G' (25 °C) (Pa × 10⁻⁷)	G' (−80 °C) (Pa × 10⁻⁹)	G'' (25 °C) (Pa × 10⁻⁶)	T_g (°C)
9/22/1	0.16	2.3	2.0	4.0	−40
9/22/2	0.16	4.2	2.0	7.1	−45
9/25/1	0.16	3.8	2.2	6.4	−45
9/5/1	0.16	2.1	1.9	3.9	−45
9/21/2	0.32	1.6	1.8	3.0	−40
8/31/2	0.32	2.3	1.5	3.6	−40
9/21/1	0.32	2.2	1.6	2.9	−35
9/4/1	0.32	2.1	1.8	3.5	−40
9/5/3	0.32	1.3	1.7	3.4	−50
L-110	0.32	1.8	1.7	2.7	−40
L-67	0.32	2.1	2.0	3.1	−40

The experimental results are given in Table III. Note that for all cases the Graetz number (G_z) is large, indicating a low heat conduction effect. The last line in Table III, designated "qualitative classification," refers to the visual inspection of the region located immediately after the object. The designation "very good" means that there is no visible knit line effect; the designation "bad" means that the knit line is completely visible.

As can be seen in Table III, there are three performance regions, depending on the value of the local Gelling number. First, if the gelling number (G_0) is larger than 0.11, the knit line is visible and weak. Second, if it is smaller than 0.07, the knit lines are strong and not visible. Last, there is a transition region between the two extreme cases. The results are shown in graphical form in Figure 3, which, as expected, shows that increasing G_0, decreases the knit line
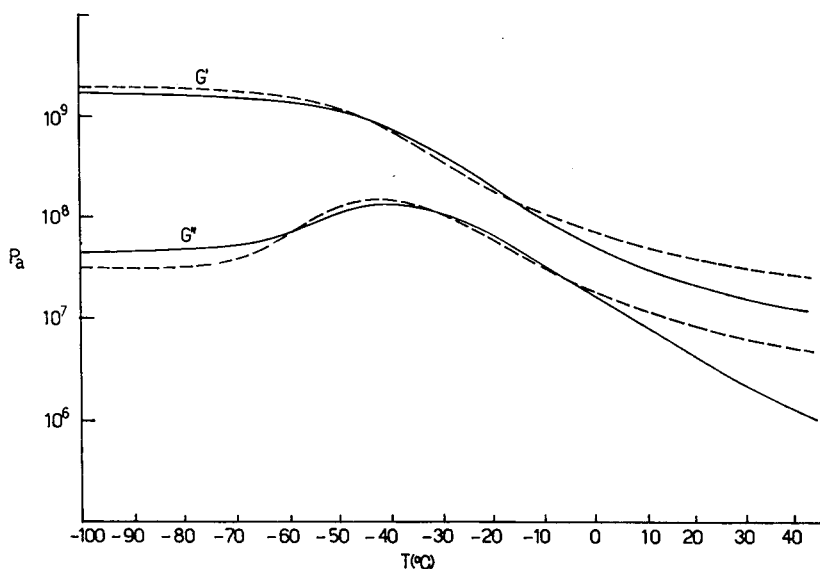

Fig. 4. Elastic shear modulus and viscous dissipation modulus for a thick and a thin sample as a function of temperature. (- - -) 0.16, 9/25/1; (—) 0.32, 9/21/2.
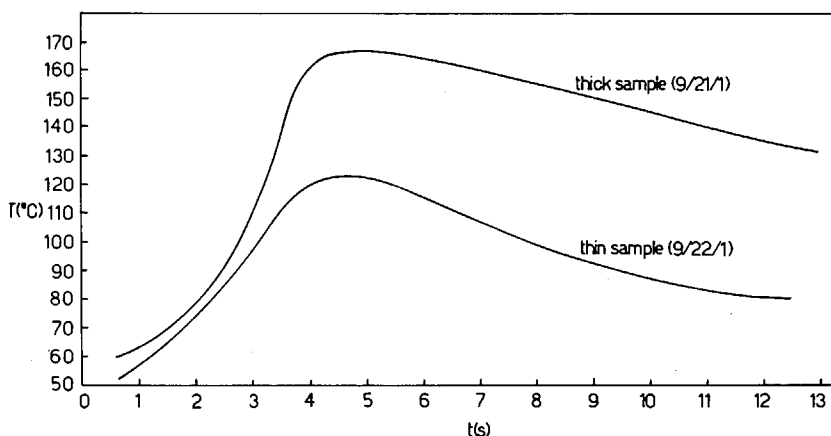
Fig. 5. Comparison of the center-line temperature rise for a thin and a thick sample.

strength. This is due to the fact that G_0 increases with increasing the conversion of the two streams meeting each other after the object, which makes their interpenetration more difficult.

Premature Gelling

The results in this section were gathered from the experiments reported by Castro and Macosko[6] by observing when premature gelling was obtained. They can be correlated to processing conditions using the gelling, number (G) and the Graetz number (G_z), which are defined as follows:

$$G = \frac{\text{filling time } (t_f)}{\text{isothermal gel time at } T_m \ (t_{gm})} \tag{2}$$

and

$$G_z = \frac{(H/2)^2}{t_f \alpha} \tag{3}$$

T_m is the average of the initial and mold wall temperature, α is the thermal diffusivity $\bar{k}/\rho C_p$, and t_{gm} is the gel time at T_m:

$$t_{gm} = (k_{T_m} C_0)^{-1} C_g^* / (1 - C_g^*) \tag{4}$$

What we found was that for the typical RIM case $(T_w > T_0)$ the gelling number at which premature gelling occurs increases as the Graetz number increases. This is due to the fact that the reaction rate is proportional to the temperature and the mold wall acts as a heat source. The lower the Graetz number, the more heat is transferred to the flowing mixture.

As a general rule, we could say that for Graetz numbers larger than 10, premature gelling could occur for gelling numbers larger than 0.17 and for Graetz numbers between 2 and 10, for values larger than 0.06. Strictly speaking, these values are applicable only for the specific chemical system that they were obtained from (RIM 2200 and experimental system), but we believe that, as long as the shape of the viscosity rise is similar, one could use the same values for a different chemical system.

Final Part Physical Properties

Extensional Properties. For each plaque as discussed in the procedures section, four samples were tested; their positions are shown in Figure 2. The complete experimental results are given in Table V. As can be seen, no significant difference was found according to the sample location for any of the properties tested. This implies that the sample is isotropic with respect to planar rotations parallel to the mold walls, which is one of the advantages of RIM with respect to thermoplastic molding. In RIM, most of the polymerization occurs after the mold is already filled; thus, there is no alignment of the macromolecule due to the flow field. In thermoplastic molding, since we inject a polymer already reacted, the macromolecule aligns in the flow direction, producing a nonisotropic part. What we do have is surface to center variations due to the very different temperature history in both locations.[3-5] The influence of mold thickness (H) and mold wall temperature (T_w) can be seen by looking at the averages per sample in Table V. We can conclude that there is not a major effect of the mold wall temperature, but, mold thickness, on the other hand, does affect the strength of the part. The thin samples (0.16 cm) gave consistently better properties than the thick ones (0.32 cm.).

Dynamic Torsion. The experimental results are summarized in Table VI. The general trend is similar to that of the extensional properties. The thin samples have larger elastic shear modulus (G') at $-80°C$ and $25°C$ and also a larger viscous modulus at $25°C$ (G''). The glass transition temperature determined from the maximum in G'' is not affected by thickness. The wall temperature again, does not affect the properties. Figure 4 shows a full comparison of G' and G'' vs. temperature for a thin (9/25/1) and a thick one (9/21/2). The trend is similar for the other samples. Note that the differences are not very large.

DISCUSSION

We have shown how using the dimensionless groups relevant to the RIM process, that is, the Gelling number (G) and the Graetz number (G_z), guide lines for "good filling" can be achieved. That is, we can obtain bounds for those parameters under which premature gelling and knit line problems are avoided. We also show that RIM parts are fairly isotropic with respect to planar rotations parallel to the mold walls. This is due to the fact that most of the polymerization occurs, after the mold is filled, that is, during the curing step. This is a major advantage of RIM with respect to thermoplastic molding, where a polymer already formed is injected into the mold, and thus the macromolecules align with the flow.

It was also found that the mold wall temperature does not greatly affect the final plaque physical properties. This is an important conclusion since, we can then vary the mold wall temperature (T_w) and optimize the filling and curing stages. We would like T_w as high as possible so as to decrease the demold time to a minimum, but not so high as to produce premature gelling or thermal degradation. The mold thickness was found to have a larger effect on the physical properties. The thinner samples gave consistently better properties than the thick ones. This can be better understood by looking at Figure 5, where the
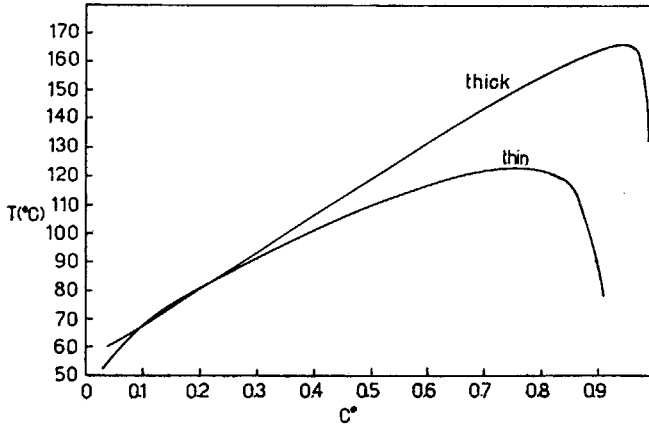
Fig. 6. Comparison of the center-line temperature conversion pathway for a thin and a thick sample.

center line temperature rise during curing for a thin and thick sample are compared. The rise for the thick sample is much larger than for the thin one, due the lower influence of the mold wall on the thick sample. The center-line rise for the thick sample is close to the adiabatic rise. Thus, the center to wall variations are larger for the thick sample while the thin sample is somewhat more homogeneous. This becomes even more evident by looking at Figure 6, where the temperature conversion pathway for both samples is analyzed. The thick sample is at a higher temperature level than the thin one during most of the reaction. We think that the fact that wall to center variations are decreased in the thin samples is responsible, at least in part, for the better properties of the thin samples.

APPENDIX: NOMENCLATURE

C	concentration of reactive species at time t
C_0	initial concentration of reactive species
C^*	extent of reaction $(C_0 - C)/C$
C_g	solidification (gel) point
C_p	heat capacity at constant pressure
E	activation energy
E_{100}	extensional modulus at 100% elongation
G'	elastic dynamic shear modulus
G''	viscous dynamic modulus
H	mold thickness
H_r	heat of reaction
k	thermal conductivity
k_0	preexponential factor in kinetic constant
k	kinetic rate constant $= k_0 e^{-E/RT}$
k_{T_m}	kinetic rate constants evaluated at T_m
T	temperature
T_0	initial material temperature
T_w	mold wall temperature
T_m	mean temperature: $(T_0 + T_w)/2$
t	time
t_f	filling time

t_{gm}	isothermal gel time at T_m
W	mold width
α	thermal diffusivity $= k/\rho C_p$
ϵ	elongation %
ρ	density
σ_b	tensil strength

Dimensionless Groups

G	gelling number
G_z	Graetz number

References

1. A. L. Chang, R. M. Briber, E. L. Thomas, R. J. Zdrahala, and F. E. Critchfield, *Polymer*, **23**, 1060 (1982).

2. J. M. Castro, C. W. Macosko, F. E. Critchfield, E. C. Steinle, and L. P. Tackett, *J. Elast. Plast.*, **12**, 3 (1980).

3. J. M. Castro, C. W. Macosko, F. E. Critchfield, E. C. Steinle, L. P. Tackett, *Soc. Plast. Eng. Tech. Pap.*, **26**, 423 (1980).

4. M. Tirrel, L. J. Lee, and C. W. Macosko, *Am. Chem. Soc. Symp. Ser.*, **104**, 149 (1979).

5. I. D. Fridman, E. L. Thomas, L. J. Lee, and C. W. Macosko, *Polymer*, **21**, 393 (1980).

6. J. M. Castro and C. W. Macosko, *AIChE J.*, **28**, 250 (1982).

7. R. J. Zdrahala, R. M. Gerkin, S. L. Hager, and F. E. Critchfield, *J. Appl. Polym. Sci.*, **24**, 2041 (1979).

8. J. M. Castro and C. W. Macosko, *Soc. Plast. Eng. Tech. Pap.*, **26**, 434 (1980).

9. L. J. Lee and C. W. Macosko, *Soc. Plast. Tech. Pap.*, **24**, 151 (1978).